A one-dimensional model of a thermosyphon with known wall temperature

M. Gordon*, E. Ramos* and M. Sen†

A model of a thermosyphon with arbitrary geometry and known wall temperature is presented. A one-dimensional study is made with axial conduction effects included. Both steady-state as well as time-dependent behaviours are analysed. Multiple steady-state solutions are identified. The time-dependent problem can be reduced to a set of infinite ordinary differential equations. However, the flow velocity is determined from a subset of three equations. These equations are closely related to the Lorenz equations.

Keywords: *thermosyphons, one-dimensional model, natural convection loops, axial thermal conduction*

Introduction

Natural convection loops have been studied extensively in recent years. Interest has arisen, on the one hand because of their importance in practical applications such as solar energy utilization[1,2], emergency nuclear reactor cooling[3,4], and heat dissipation from electrical components, and on the other because natural convective loops are devices that can be described with simple one-dimensional models that display fundamental properties of natural convection phenomena like multiplicity of steady-state solutions and periodic oscillations; see for instance Refs 5–8. A recent review on natural circulation loops is presented by Mertol and Greif[9].

Using Fourier analysis as proposed by Malkus[10], Yorke and Yorke[6] studied the convective motion inside a toroidal one-dimensional loop, assuming known wall temperature but neglecting axial heat conduction. They found that the velocity in the transient state can be described by a set of three ordinary differential equations that for symmetric heating reduce to the Lorenz equations[11]. The fluid motion was found to display steady, periodic and aperiodic behaviour.

Up to now, thermal axial conduction has been neglected in most theoretical analyses. Although this effect is unimportant in some practical applications, it can be the dominant effect when the working fluid has large thermal conductivity. The effect of axial conduction on the velocity and temperature distribution in a toroidal loop with constant heat input in the lower half and known wall temperature in the upper half was numerically investigated by Greif *et al*[12], who reached the conclusion that it stabilizes the flow and smoothens out temperature fields. In an investigation carried out in parallel with the present paper, Sen *et al*[13] have theoretically studied the convective flow inside a loop of arbitrary geometry and known heat input. Application of the theory developed by them to a toroidal geometry indicates that the steady-state velocity as a function of the tilt angle and the heat flux has the properties of a cusp catastrophe. Also, it is emphasized that zero velocity can be a steady-state solution in contrast with the case of no axial conduction.

In the present paper, we study the convective motion inside a loop with arbitrary geometry and known wall temperature; axial heat conduction is taken into account. The particular case of toroidal geometry is studied in detail.

* Laboratorio de Energía Solar, Instituto de Investigaciones en Materiales, Universidad Nacional Autónoma de México, 62580 Temixco, Mor., Mexico
† Depto. de Fluidos y Térmica, Facultad de Ingeniería, Universidad Nacional Autónoma de México, 04510 México, D.F., Mexico
Manuscript received 18 July 1985 and accepted for publication 21 July 1986

0142-727X/87/030177-05$3.00

Mathematical formulation

A thermosyphon of arbitrary configuration but with smooth bends of a large radius compared with that of the pipe, and constant cross-section, contained in a vertical plane is considered. A known wall temperature $T_w(s)$ over the entire loop is assumed, where s is a longitudinal coordinate (Fig 1). The convective heat transfer coefficient h is taken to be a constant. The one-dimensional equations are used together with the Boussinesq approximation. Axial conduction is included, and viscous dissipation is neglected as are the effects of curvature.

From the equation of continuity for incompressible flow, we have that the velocity is a function of time only. The momentum equation in the s direction is given by

$$\rho \frac{du}{dt} = -\frac{\partial p}{\partial s} - \rho \tilde{g}(s) - \frac{32\nu}{D^2} u \tag{1}$$

where $\tilde{g}(s)$ is the component of the gravitational acceleration in the negative longitudinal direction. The friction forces are taken to correspond to fully developed Poiseuille flow. The flow is induced by the density field $\rho(T)$, which we assume to be a linear

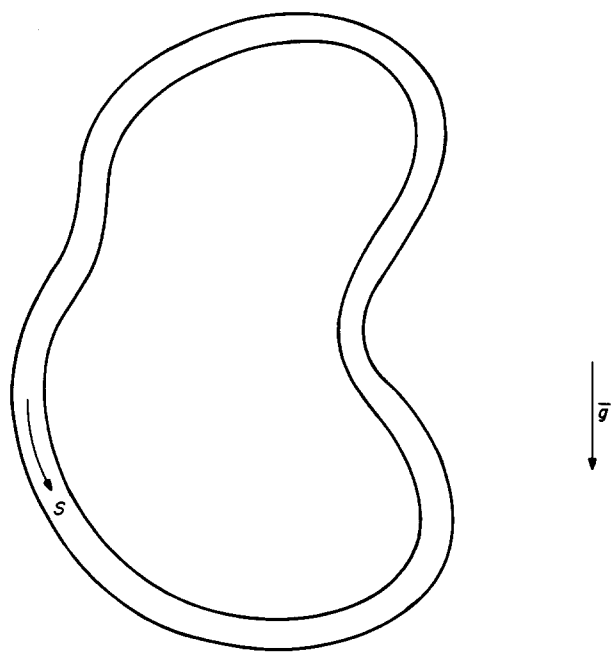

Figure 1 The natural circulation loop. The wall temperature is a known function of the longitudinal coordinate s

function of the form

$$\rho=\rho_0\{1-\beta(T-T_0)\}$$

where ρ_0 is the fluid density at the reference temperature T_0 and β is the volumetric expansion coefficient.

Using the expression for the density in terms of the temperature in Eq (1), and integrating around the loop, we get

$$\frac{du}{dt}+\frac{32\nu}{D^2}u=\frac{\beta}{L}\int_0^L \tilde{g}(s)T(s,t)\,ds \tag{2}$$

The energy equation is

$$\frac{\rho_0 cD}{4}\left(\frac{\partial T}{\partial t}+u\frac{\partial T}{\partial s}\right)=\frac{kD}{4}\frac{\partial^2 T}{\partial s^2}+h(T_w-T) \tag{3}$$

The solution for the velocity and the temperature are obtained by solving Eqs (2) and (3) simultaneously.

The dimensionless forms of the governing equations are:

$$\frac{dV}{d\tau}+V=G\int_0^1 \delta(x)\theta(x,\tau)\,dx \tag{4}$$

and

$$\frac{\partial\theta}{\partial\tau}+V\frac{\partial\theta}{\partial x}-K\frac{\partial^2\theta}{\partial x^2}+H\theta=H\theta_w \tag{5}$$

where the dimensionless parameters are defined in the Notation.

Steady-state solutions

Indicating the time-independent variables by $\bar{V}$ and $\bar{\theta}(x)$, the steady-state governing equations (4) and (5) simplify to

$$\bar{V}=G\int_0^1 \delta(x)\bar{\theta}(x)\,dx \tag{6}$$

and

$$\bar{V}\frac{\partial\bar{\theta}}{\partial x}-K\frac{\partial^2\bar{\theta}}{\partial x^2}+H\bar{\theta}=H\bar{\theta}_w \tag{7}$$

Integrating Eq (7), and using the boundary conditions

$$\bar{\theta}(0)=\bar{\theta}(1)$$

$$\left.\frac{d\bar{\theta}}{dx}\right|_{x=0}=\left.\frac{d\bar{\theta}}{dx}\right|_{x=1}$$

the temperature distribution becomes

$$\begin{aligned}\bar{\theta}=-\frac{b}{r_2-r_1}\Bigg\{&\frac{\exp(r_1+r_1x)}{1-\exp(r_1)}\int_0^1\exp(-r_1x)\bar{\theta}_w(x)\,dx\\&-\frac{\exp(r_2+r_2x)}{1-\exp(r_2)}\int_0^1\exp(-r_2x)\bar{\theta}_w(x)\,dx\\&+\exp(r_1x)\int_0^x\exp(-r_1x')\bar{\theta}_w(x')\,dx'\\&-\exp(r_2x)\int_0^x\exp(-r_2x')\bar{\theta}_w(x')\,dx'\Bigg\}\end{aligned} \tag{8}$$

where

$$r_1=-\frac{a}{2}-\frac{1}{2}\sqrt{a^2-4b}$$

$$r_2=-\frac{a}{2}+\frac{1}{2}\sqrt{a^2-4b}$$

$$a=-\bar{V}/K$$

$$b=-H/K$$

Toroidal thermosyphon

We consider the special case of a toroidal geometry. The wall temperature is assumed to be

$$\bar{\theta}_w=-\sin(2\pi x-\gamma)$$

where γ is an angle of inclination. When $\gamma=0$, the wall temperature is symmetric with respect to a vertical diameter.

Replacing $\bar{\theta}_w$ in Eq (8), and integrating, we get

$$\begin{aligned}\bar{\theta}=\frac{b}{r_2-r_1}\Bigg\{&\frac{\cos(2\pi x-\gamma)}{2\pi(1+r_2^2/4\pi^2)}-\frac{\cos(2\pi x-\gamma)}{2\pi(1+r_1^2/4\pi^2)}\\&+\frac{r_2\sin(2\pi x-\gamma)}{4\pi^2(1+r_2^2/4\pi^2)}-\frac{r_1\sin(2\pi x-\gamma)}{4\pi^2(1+r_1^2/4\pi^2)}\Bigg\}\end{aligned} \tag{9}$$

The gravity function that corresponds to a toroidal thermosyphon is

$$\delta(x)=\cos(2\pi x) \tag{10}$$

using Eqs (9) and (10) in Eq (6), we get an expression for the

Notation

B_1	Parameter defined after Eq (27)
B_2	Parameter defined after Eq (27)
c	Specific heat
D	Internal diameter
G	Gr/α
$\bar{g}$	Gravitational acceleration
$\tilde{g}$	Local component of gravitational acceleration
Gr	Grashof Number $\equiv\beta\Delta Tg D^3/1024\nu^2$
H	Nu/Pr
h	Heat transfer coefficient
K	$1/(Pr\,\alpha^2)$
k	Heat conductivity
L	Total length of the loop
Nu	Nusselt Number $\equiv 4Dh/k$
p	Pressure
Pr	Prandtl Number $\equiv 32\rho_0 c\nu/k$
s	Longitudinal coordinate
T	Temperature
t	Time
u	Velocity
V	Dimensionless velocity $\equiv D^2u/32\nu L$
x	Dimensionless longitudinal coordinate $\equiv s/L$
X	Variable representing dimensionless velocity V in Eqs (25)–(27)
Y	$G\theta_1^c$ (in Eqs (25)–(27))
Z	$G\theta_1^s$ (in Eqs (25)–(27))
α	L/D
β	Coefficient of volumetric expansion
γ	Angle of inclination
δ	Dimensionless local gravitational acceleration $\equiv\tilde{g}/g$
ΔT	Reference temperature difference
ε	Parameter defined after Eq (11)
θ	Dimensionless temperature $\equiv(T-T_w)/\Delta T$
λ	$4\pi^2K+H$
ν	Kinematic viscosity
ξ	Parameter defined after Eq (11)
ρ	Density
σ	$1/\lambda$
τ	Dimensionless time $\equiv 32\nu t/D^2$

Subscripts and superscripts

c	Cosine coefficiency
o	Reference value
s	Sine coefficient
w	Value at the wall
$\bar{}$	Time independent values
$'$	Variables defined after Eq (27)

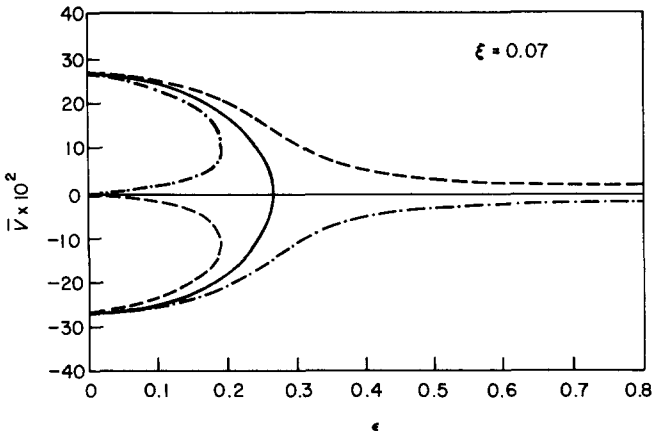

Figure 2 Steady-state velocity $\bar{V}$ as a function of ε for $\xi=0.07$; ——, $\gamma=0$; – – – – $\gamma=10°$; – · – · – · – $\gamma=-10°$

velocity

$$\bar{V}=\frac{GH\{2\pi\bar{V}\cos\gamma+(4\pi^2K+H)\sin\gamma\}}{2\{(4\pi^2K+H)^2+(2\pi\bar{V})^2\}} \tag{11}$$

Making the following change of variables:

$$\xi=GH/4\pi$$

and

$$\varepsilon=(4\pi^2K+H)/2\pi$$

we obtain

$$\bar{V}=\frac{\xi}{\varepsilon^2+\bar{V}^2}(\bar{V}\cos\gamma+\varepsilon\sin\gamma) \tag{12}$$

the solutions of which give the steady-state velocity for the toroidal thermosyphon. Fig 2 shows $\bar{V}$ as a function of ε for a fixed ξ and $\gamma=0°\pm10°$. In general, three complex solutions may be found. In the particular case $\gamma=0°$, where heating takes place on the lower half and cooling on the upper half, the solutions are: $\bar{V}=0\pm\sqrt{\xi-\varepsilon^2}$.

For fixed heat transfer coefficient and Grashof number, large heat conductivities such that $\varepsilon^2>\xi$ yield $\bar{V}=0$ as the only possible real solution, while for $\varepsilon^2<\xi$ three real solutions may occur. This result is expected since, for the first case, the heat can be transferred from the hot to the cold region entirely by conduction. In the second case with low conductivity the more efficient heat transport mechanism of convection appears. The same comments apply for a tilted thermosyphon for either positive or negative (small) angles, as can be seen from Fig 2. When $\gamma\neq0$, strict zero velocity is not present for finite ε, but a sharp decrease in the velocity is found, indicating that conduction is the dominant heat transport mechanism for large ε. For a given heat transfer coefficient and working fluid, existence of the nontrivial solution for the steady-state velocity depends on the Grashof number or, equivalently, on the heat input. Fig 3 shows the velocity as a function of the tilt angle for fixed ξ and $\varepsilon=0.1$, 0.2 and 0.3. It can be seen that, for large tilt angles, only one real solution is obtained.

Transient state

We now analyse the transient behaviour of a thermosyphon of arbitrary shape. Because $\delta(x)$, $\theta(x,\tau)$ and $\theta_w(x)$ are periodic, we can make the following Fourier series expansions:

$$\delta(x)=\sum_{n=1}^{\infty}\{\delta_n^c\cos2\pi nx+\delta_n^s\sin2\pi nx\} \tag{13}$$

$$\theta(x,\tau)=\theta_0(\tau)+\sum_{n=1}^{\infty}\{\theta_n^c(\tau)\cos2\pi nx+\theta_n^s(\tau)\sin2\pi nx\} \tag{14}$$

$$\theta_w(x)=\theta_{w,0}+\sum_{n=1}^{\infty}\{\theta_{w,n}^c\cos2\pi nx+\theta_{w,n}^s\sin2\pi nx\} \tag{15}$$

where

$\theta_0(\tau)$ is the spatial average of the dimensionless fluid temperature:

$$\theta_0(\tau)=\int_0^1\theta(x,\tau)\,dx$$

and $\theta_{w,0}$ is the spatial average of the dimensionless wall temperature:

$$\theta_{w,0}=\int_0^1\theta_w(x)\,dx$$

Introducing Eqs (13) and (14) to Eq (4), and simplifying, we get

$$\frac{dV}{d\tau}+V=G\int_0^1\left[\sum_{n=1}^{\infty}\{\delta_n^c\cos2\pi nx+\delta_n^s\sin2\pi nx\}\times\sum_{n=1}^{\infty}\{\theta_n^c(\tau)\cos2\pi nx+\theta_n^s(\tau)\sin2\pi nx\}\right]dx \tag{16}$$

From Eq (5) we have

$$\frac{d\theta}{d\tau}-H(\theta_{w,0}-\theta_0)+\sum_{n=1}^{\infty}\left\{\frac{d\theta_n^c}{d\tau}\cos2\pi nx+\frac{d\theta_n^s}{d\tau}\sin2\pi nx\right\}-2\pi V\sum_{n=1}^{\infty}\{n\theta_n^c\sin2\pi nx-n\theta_n^s\cos2\pi nx\}+4\pi^2K\sum_{n=1}^{\infty}\{n^2\theta_n^c\cos2\pi nx+n^2\theta_n^s\sin2\pi nx\}=H\sum_{n=1}^{\infty}\{\theta_{w,n}^c\cos2\pi nx+\theta_{w,n}^s\sin2\pi nx\}-H\sum_{n=1}^{\infty}\{\theta_n^c(\tau)\cos2\pi nx+\theta_n^s(\tau)\sin2\pi nx\} \tag{17}$$

Integrating this around the loop, we get

$$\frac{d\theta_0}{d\tau}=H(\theta_{w,0}-\theta_0) \tag{18}$$

the solution of which with initial condition $\theta_0(0)$ is

$$\frac{\theta_{w,0}-\theta_0(\tau)}{\theta_{w,0}-\theta_0(0)}=\exp(-H\tau) \tag{19}$$

From Eq (17), we get

$$\frac{d\theta_m^c}{d\tau}+2\pi mV\theta_m^s+4\pi^2m^2K\theta_m^c=H(\theta_{w,m}^c-\theta_m^c) \tag{20}$$

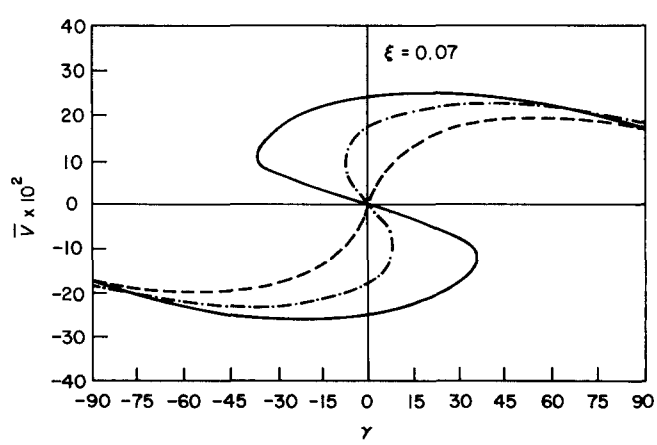

Figure 3 Steady-state velocity $\bar{V}$ as a function of the tilt angle γ; —— $\varepsilon=0.1$; – · – · – $\varepsilon=0.2$; – – – – $\varepsilon=0.3$

Table 1 Physical properties of three liquids considered

	Acetone	Water	Mercury
ρ_0 (kg m^{-3})	791	998	13 546
β (°C^{-1})	14.3×10^{-4}	1.8×10^{-4}	1.8×10^{-4}
c (J kg^{-1}°C^{-1})	2.16×10^{3}	4.18×10^{3}	0.14×10^{3}
k (W m^{-1}°C^{-1})	0.180	0.598	9.304
ν (m^2 s^{-1})	4.18×10^{-7}	10.06×10^{-7}	1.15×10^{-7}

and

$$\frac{d\theta_m^s}{d\tau}-2\pi mV\theta_m^c+4\pi^2m^2K\theta_m^s=H(\theta_{w,m}^s-\theta_m^s) \tag{21}$$

The equations (16), (20) and (21) represent an infinite set of ordinary differential equations in the unknowns $V(\tau)$, $\theta_0(\tau)$, $\theta_m^c(\tau)$, $\theta_m^s(\tau)$, $(m=1,2,\ldots)$. For the toroidal geometry, $\delta(x)=\cos(2\pi x)$ and the velocity $V(\tau)$ is determined by a subset of three equations which decouple from the rest. These are

$$\frac{dV}{d\tau}+V=\frac{G}{2}\theta_1^c \tag{22}$$

$$\frac{d\theta_1^c}{d\tau}+2\pi V\theta_1^s+4\pi^2K\theta_1^c=H(\theta_{w,1}^c-\theta_1^c) \tag{23}$$

$$\frac{d\theta_1^s}{d\tau}-2\pi V\theta_1^c+4\pi^2K\theta_1^s=H(\theta_{w,1}^s-\theta_1^s) \tag{24}$$

If we make a change of variables of the following form:

$$X=V$$

$$Y=\frac{G}{2}\theta_1^c$$

$$Z=\frac{G}{2}\theta_1^s$$

then Eqs (22)–(24) become

$$\frac{dX}{d\tau}=Y-X \tag{25}$$

$$\frac{dY}{d\tau}=B_1-2\pi XZ-\lambda Y \tag{26}$$

$$\frac{dZ}{d\tau}=-B_2+2\pi XY-\lambda Z \tag{27}$$

where

$$B_1=\frac{G}{2}H\theta_{w,1}^c$$

$$B_2=-\frac{G}{2}H\theta_{w,1}^s$$

$$\lambda=4\pi^2K+H$$

With the further change of variables

$$X'=X/\lambda$$

$$Y'=2\pi Y/\lambda$$

$$Z'=\frac{2\pi}{\lambda}(Z+B_2/\lambda)$$

and

$$\tau'=\lambda\tau$$

Eqs (25)–(27) take the form

$$\frac{dX'}{d\tau'}=\sigma(Y'-X') \tag{28}$$

$$\frac{dY'}{d\tau'}=-Y'+rX'-Z'X'+R' \tag{29}$$

$$\frac{dZ'}{d\tau'}=X'Y'-Z' \tag{30}$$

with

$$\sigma=1/\lambda$$

$$r=2\pi B_2/\lambda^2$$

$$r'=2\pi B_1/\lambda^2$$

For a symmetrical distribution of the wall temperature around a vertical diameter $\theta_{w,1}^c=0$, $B_1=0$, for which $r'=0$. Eqs (28)–(30) then reduce to the Lorenz equations, whose properties have been discussed thoroughly elsewhere[6,11].

Particular examples

In order to visualize the results obtained in the previous section, the stability of the flows of three working fluids in toroidal loops are discussed. The chosen fluids are acetone, water and mercury. The wall temperature is assumed to be of the form $\theta_{w,1}^c=0$, $\theta_{w,1}^s=-1$ and therefore symmetrical with respect to the vertical. Under these conditions, $r'=0$ in Eq (29). The heat transfer coefficient, required to calculate the Nusselt number, is taken as

$$h=1\ \text{J m}^{-2}\,\text{s}^{-1}\,\text{°C}^{-1}$$

The temperature for $s=0$ is 20°C. The physical properties of the fluids are given in Table 1.

The stability maps in the $(1/\alpha, \Delta T)$ space for the cases under study are given in Fig 4. According to the Lorenz equation theory[6,11] the stability boundaries are given by the following expressions.

(i) For $\sigma>2$:

- $r<1$, one stable conductive solution, region (1);
- $1<r<\dfrac{\sigma(\sigma+4)}{\sigma-2}$, two stable solutions, region (2);
- $r>\dfrac{\sigma(\sigma+4)}{\sigma-2}$, unstable solutions, region (3).

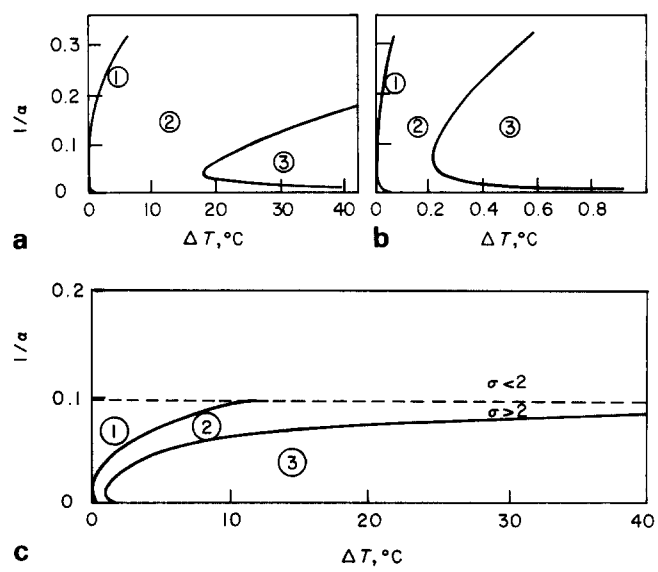

Figure 4 Stability maps for (a) acetone, (b) water and (c) mercury; d=0.01 m; h=1 J m^{-2} s^{-1}°C^{-1}. Region (1) $r<1$; Region (2) $1<r<(\sigma(\sigma+4)/(\sigma-2))$; (3) $r>(\sigma(\sigma+4)/(\sigma-2))$

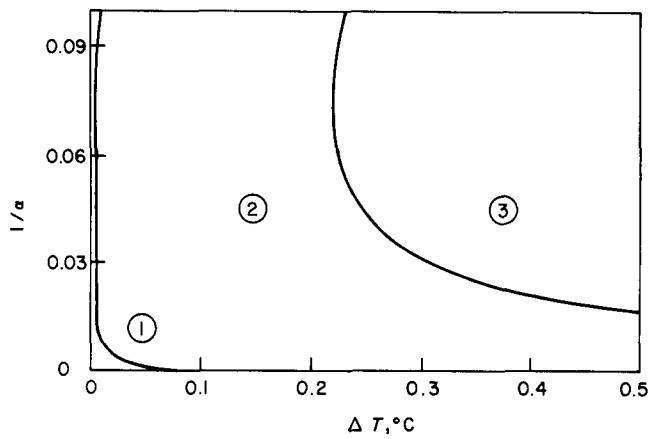

Figure 5 Stability map for a fictitious fluid with physical properties as those of mercury, but thermal conductivity $10^{-6}\,W\,m^{-1}°C^{-1}$

(ii) For $\sigma < 2$ the system is motionless.

The geometrical parameter $1/\alpha$ (cross-sectional diameter/total length of the torus) is used in the vertical axis, and therefore the possible values go from zero to $1/\pi$. The lower region corresponds to long, thin loops, while the upper region corresponds to fat loops. The one-dimensional theory presented here is expected to be valid for the lower part of the maps, since no two- or three-dimensional effects, which might be dominant for fat loops, are taken into account.

It is clearly seen that all examples are stable for low ΔT, as they are expected to be. Actually, $\Delta T = 0$ should be stable for all geometries. Also, in the limit $1/\alpha \to 0$ the systems are stable since the frictional effects are dominant. The unstable region for the acetone is larger than that of water. This is expected since the acetone has a larger thermal expansion coefficient and lower kinematic viscosity than water. Thin loops with mercury as working fluid are found to be unstable for ΔT as small as 0.1°C but very large temperature differences ($\Delta T \sim 50°C$) are required for $1/\alpha > 0.1$. In order to clarify the role played by the thermal conductivity in this case, Fig 5 shows the stability map obtained for a fictitious fluid with the same properties as the mercury, but with a thermal conductivity $k = 10^{-6}\,W\,m^{-1}°C^{-1}$. The effect is that, except for a small region at extremely low ΔT or $1/\alpha$, the system in motion.

Conclusions

The effect of axial heat conduction on a one-dimensional loop with known wall temperature is analysed. Multiple steady-state velocities are found, the values of which depend on the geometry of the loop, the heat input and the physical properties of the working fluid. The qualitative nature of the steady-state velocity for both the conductive and nonconductive models is similar. This is also true for the transient governing equations, which have the same qualitative nature for both models. For this reason the nonconducting model as discussed in Ref 6 is structurally stable.

References

1 Norton, B. and Probert, S. D. Natural circulation solar-energy stimulated systems for heating water. *Appl. Energy*, 1982, **11**, 167–196

2 Norton, B. and Probert, S. D. Thermosyphonic water heaters stimulated by renewable energy sources. *Appl. Energy*, 1982, **12**, 237–242

3 Agrawal, A. K., Madni, I. K., Guppy, J. G. and Weaver, W. L. Dynamic simulation of LMFBR plant under natural circulation. *J. Heat Transfer*, 1981, **103**, 312–318

4 Grand, D. *Natural Convection Cooling in Nuclear Reactor Safety*, ed. O.C. Jones, Hemisphere Publishing Corp. New York, 1983, 729–750

5 Crevelling, H. F., de Paz, J. F., Baladi, J. Y. and Schoenhals, R. J. Stability characteristics of a single-phase free convection loop. *J. Fluid Mech.*, 1975, **67**, 65–84

6 Yorke, J. A. and Yorke, G. D. Chaotic behavior and fluid dynamics. In *Hydrodynamic Instabilities and the Transition to Turbulence*, eds H. L. Swinney and J. P. Gollub, Springer-Verlag, Berlin, 1981

7 Hart, J. E. A new analysis of a closed loop thermosyphon. *Int. J. Heat Mass Transfer*, 1984, **27**, 125–136

8 Sen, M., Ramos, E. and Treviño, C. Natural convective loop with known heat flux. *Int. J. Heat Mass Transfer*, 1985, **28**(1), 219–233

9 Mertol, A. and Greif, R. A review of natural circulation loops. In Proc. NATO Advanced Study Institute on Natural Convection: Fundamentals and Applications, Turkey 1984. Also in *Natural Convection: Fundamentals and Applications*, eds W. Aung, S. Kakac and R. Viskanta, Hemisphere Publishing Corp. New York, to be published.

10 Malkus, W. V. R. Non-periodic convection at high and low Prandtl number. *Mémoires Societé Royale des Sciences de Liége*, 1972, **69**, Tome IV, 125–128

11 Lorenz, E. N. Deterministic non-periodic flow. *J. Atmos. Sci.*, 1963, **29**, 130–141

12 Greif, R., Zvirin, Y. and Mertol, A. The transient and stability behavior of a natural convection loop. *J. Heat Transfer*, 1979, **101**, 684–688

13 Sen, M., Ramos, E., Treviño, C. and Salazar, O. One-dimensional analysis of thermosyphons with axial conduction effects. Submitted for publication

14 Stewart, I. Catastrophe theory in physics. *Progress Reports in Physics*, 1982, **45**